A Spiking Neuron and Population Model based on the Growth Transform Dynamical System

Ahana Gangopadhyay[1], Darshit Mehta[2], and Shantanu Chakrabartty[1]

[1]Department of Electrical and Systems Engineering, Washington University in St. Louis
[2]Department of Biomedical Engineering, Washington University in St. Louis

Abstract

This paper introduces a new spiking neuron model based on the Growth transform dynamical system, where the process of spike generation and encoding results from the optimization of a network/population energy functional. As a result, the population-level spiking dynamics are always stable and interpretable. In this paper, we show how the model can be configured to generate a wide range of neural dynamics reported in literature by modulating the model hyperparameters in a manner that the network objective function, or the optimized solution of the system remains unaffected. A publicly available software tool implementing the proposed model can be used to explore a number of single-cell and population dynamics under different conditions and network configurations, and could serve as an important framework for building scalable, energy-efficient neuromorphic machine learning algorithms.

Keywords— Spiking neuron model, Growth transform dynamical system, energy minimization, neural dynamics, population model.

1 Introduction

The nervous system - from the cellular level to neural ensembles - has been studied extensively within the context of dynamical systems [1], modeled as a set of differential equations that govern the temporal evolution of its state variables. For a single neuron, the state variables are usually its membrane potential and the conductances of ion-channels that mediate changes in the membrane potential via flux of ions across the cell membrane. A vast body of literature, ranging from the classical Hodgkin-Huxley model [2], FitzHugh-Nagumo model [3], Izhikevich model [4] to simpler integrate-and-fire models [5], treats the problem of single-cell excitability at various levels of detail and biophysical plausibility. For neural ensembles, the state variables may be individual membrane potentials or mean firing rates that represent the collective behavior of populations of neurons, as in neural mass models like Wilson-Cowan [6], Janset-Rit [7], etc.

Physical processes occurring in nature have an universal tendency to move towards a minimum-energy state defined by the values taken by the process variables, that is a function of the inputs and the state of the process. In this regard, a prevailing hypothesis in neuroscience is that a biological network can be modeled as an unified dynamical system where the spiking activity of populations of neurons results from an emergent behavior of an underlying optimization process. For instance, this underlying process could optimize some network-level metric (for example, system energy), while satisfying physical constraints imposed by evolution and biology. This hypothesis has resulted in several optimization-based approaches which include coupled-oscillator models [8], reservoir-based approaches [9] and other statistical physics based approaches [10], to design neural dynamical systems that exhibit a rich set of trajectories. [11] takes another approach by considering an energy-function of spike-based network states, where

Summary of the Growth Transform Spiking Neuron Model

$$\frac{1}{f_i(t)}\frac{dv_i(t)}{dt} + v_i(t) = g_i\big(v_i(t)\big), \quad i = 1, \dots, N, \text{ where}$$

$$g_i(v_i(t)) = \frac{-\sum_{j=1}^{N} Q_{ij} v_j(t) + b_i(t) - \psi\big(v_i(t)\big) + \lambda v_i(t)}{-\sum_{j=1}^{N} Q_{ij} v_j(t) v_i(t) + b_i(t) v_i(t) - v_i(t)\psi(v_i(t)) + \lambda}$$

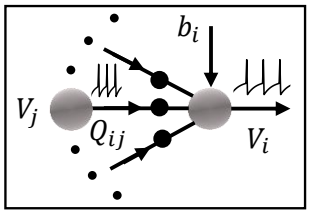

N - number of neurons; $\boldsymbol{Q}$: $\mathbb{R}^N \times \mathbb{R}^N$ - synaptic weight matrix; $\boldsymbol{b}$: $\mathbb{R}^N$ - vector of external stimulus

Modulation function, $f_i(t) = \begin{cases} f, & v_i(t) < 0 \\ 1, & v_i(t) \geq 0 \end{cases}$, $f \in [0,1]$; Spiking function, $\psi(v_i(t)) = \begin{cases} \Delta, & v_i(t) > 0 \\ 0, & v_i(t) \leq 0 \end{cases}$

Figure 1: A brief summary of the model, with relevant notations and functional forms used in the paper.

individual neuron states are assumed to be binary in nature (spiking or not spiking). However, there is a lack of an unified model in literature that treats the spike generation process as the direct derivative of optimizing an energy functional of continuous-valued neural variables (e.g. membrane potential), that can moreover be used to mimic known neural dynamics from literature.

In [12], we proposed a model of a growth transform (GT) neuron whose dynamical and spiking responses were shown to be strongly coupled with the network objective function. It was shown that while each individual neuron traverses a trajectory in the dual optimization space, the overall network traverses a trajectory in an equivalent primal optimization space. As a result, the network of growth transform neurons was shown to solve binary classification tasks, while producing stable, unique but interpretable neural dynamics like noise-shaping, spiking and bursting. In this paper, we generalize this framework to describe the model of a spiking neuron whose responses are similarly derived from minimizing a network objective function and which is flexible enough to incorporate neurodynamics that have been experimentally observed [13]. We first introduce a dynamical system of first-order differential equations based on growth transforms that maximizes a Lipschitz continuous objective function when the optimization variables are bounded, and present a proof of convergence. We then introduce a form of the energy function for a non-spiking variant of a neuron model based on this dynamical system, and extend it to a spiking variant that stochastically minimizes the network energy over a window of time. The model integrates two different dynamics - the dominant dynamics that determines the fixed-point solution of the network objective, and a modulating dynamics that controls the trajectory followed by the neuron to converge to the fixed-point solution. The latter can be tuned in a multitude of ways to program the neuron to exhibit different neural dynamics and response characteristics without affecting the underlying energy minimization process. The framework can be easily extended to implement a network of coupled neurons that can exhibit memory, global adaptation, and many more population dynamics under different initial conditions and based on different network states. For the ease of exposition, a summary of the proposed spiking neuron model is described in Fig. 1 and the rest of paper presents the derviation of this model, along with some examples of different dynamics that could be generated using this model. This paper is also accompanied by a software implementation of the model (implemented in MATLAB) and is publicly available through the web-portal at aimlab.seas.wustl.edu. Users can experiment with this software with different inputs and network parameters to create other unique dynamics.

The paper is organized as follows. Section 2 presents the growth-transform based dynamical system, along with an outline of the proof of its convergence. Section 3 presents the non-spiking

growth transform neuron model based on this dynamical system, and Section 4 extends it to a spiking neuron model. Section 5 illustrates how the proposed model can be tuned to exhibit different neural dynamics at the cellular level, as well as when several neurons are connected together through synaptic weights to form a network. Finally in Section 6, we conclude this paper with a discussion about the scope of future research in this area.

2 Growth transform dynamical system

For the ease of exposition, we first present the dynamical system model based on scalar functions and variables before extending it to the domain of vectors. Also, to simplify the mathematical notations, we will interchangeably use the continuous-time and and discrete-time representations $v(t) \in \mathcal{R}$ as $v(t) \equiv v_n$, where $n \in \mathcal{N}$ denotes the discrete-time index. Similarly, $\frac{dv}{dt} \equiv \Delta v_n = v_{n+1} - v_n$.

Theorem. Let $\mathcal{H}(v_n) : \mathcal{R} \rightarrow \mathcal{R}$ be a Lipschitz-continuous function of v_n, and let $\lambda > |\frac{\partial \mathcal{H}}{\partial v_n}|$, where λ is a hyper-parameter. If $f_n \in [0, 1]$ denotes a time-varying function, then for $|v_0| < 1$, the dynamical system

$$\frac{1}{f_n}\Delta v_n + v_n = \frac{\frac{\partial \mathcal{H}}{\partial v_n} + \lambda v_n}{v_n \frac{\partial \mathcal{H}}{\partial v_n} + \lambda} \tag{1}$$

satisfies the following criteria for all n:

$$(a)\ \mathcal{H}(v_n) \geq \mathcal{H}(v_{n-1}) \tag{2}$$

$$(b)\ |v_n| < 1 \tag{3}$$

$$(c)\ \lim_{n \rightarrow \infty}\ (v_n^2 - 1)\frac{\partial \mathcal{H}}{\partial v_n} \rightarrow 0. \tag{4}$$

Proof. We can decompose the scalar variable v_n as $v_n = v_n^+ - v_n^-$, where $v_n^+, v_n^- \geq 0$. The following additional constraint

$$v_n^+ + v_n^- = 1 \tag{5}$$

imposed on the variables v_n^+ and v_n^- would always ensure that (b) is satisfied. Then we can write

$$\arg\max_{v}\ \mathcal{H}(v) \equiv \arg\max_{v^+, v^-}\ \mathcal{H}(v^+ - v^-). \tag{6}$$

We can solve the equivalent optimization problem under the linear constraint specified by (5) using an iterative multiplicative update called growth transforms - a fixed point algorithm for optimizing any Lipschitz continuous objective function under similar equality constraints [14, 15].

The homotopically increasing property of growth transforms [16] leads to the following discrete-time update equations for the new optimization variables for maximizing $\mathcal{H}$

$$v_{n+1}^+ = (1 - f_n)v_n^+ + f_n \frac{v_n^+}{\mu_n}(\frac{\partial \mathcal{H}}{\partial v_n^+} + \lambda) \tag{7}$$

$$v_{n+1}^- = (1 - f_n)v_n^- + f_n \frac{v_n^-}{\mu_n}(\frac{\partial \mathcal{H}}{\partial v_n^-} + \lambda) \tag{8}$$

where $0 \leq f_n \leq 1$, and

$$\mu_n = v_n^+(\frac{\partial \mathcal{H}}{\partial v_n^+} + \lambda) + v_n^-(\frac{\partial \mathcal{H}}{\partial v_n^-} + \lambda) \tag{9}$$

is a normalization factor that ensures $v_{n+1}^+ + v_{n+1}^- = 1$. From (7) and (8), using $v_n = v_n^+ - v_n^-$ and (5), we can easily show

$$v_{n+1} = (1 - f_n)v_n + f_n \frac{\frac{\partial \mathcal{H}}{\partial v_n} + \lambda v_n}{v_n \frac{\partial \mathcal{H}}{\partial v_n} + \lambda} \tag{10}$$

where we have used the relation $\frac{\partial \mathcal{H}}{\partial v} = \frac{\partial \mathcal{H}}{\partial v^+} = -\frac{\partial \mathcal{H}}{\partial v^-}$. Rearranging the terms in (10), we can write

$$\begin{aligned} \tfrac{1}{f_n} \quad & [v_{n+1} - v_n] + v_n = \frac{\frac{\partial \mathcal{H}}{\partial v_n} + \lambda v_n}{v_n \frac{\partial \mathcal{H}}{\partial v_n} + \lambda}, \text{ or} \\ \tfrac{1}{f_n} \quad & \Delta v_n + v_n = \frac{\frac{\partial \mathcal{H}}{\partial v_n} + \lambda v_n}{v_n \frac{\partial \mathcal{H}}{\partial v_n} + \lambda}. \end{aligned} \tag{11}$$

This dynamical system model, derived from the growth transform updates outlined in (7) and (8), ensures that (a) holds, with equality being satisfied iff v_n is a critical point of $\mathcal{H}$. In the limit when the network reaches steady-state, using $\lim_{n\to\infty} v_{n+1} = v_n$, we have

$$\lim_{n\to\infty} v_n = \frac{\frac{\partial \mathcal{H}}{\partial v_n} + \lambda v_n}{v_n \frac{\partial \mathcal{H}}{\partial v_n} + \lambda}. \tag{12}$$

Rearranging the terms, we get (c). This guarantees that in steady-state, as long as the responses are bounded, the gradient $\frac{\partial \mathcal{H}}{\partial v_n}$ goes to zero.

Extending this to a vector dynamical system where $\mathcal{H} : \mathcal{R}^N \to \mathcal{R}$ is a function of $\boldsymbol{v}_n = \{v_{1,n}, v_{2,n}, .., v_{N,n}\}$, we can write

$$\frac{1}{f_{i,n}} \Delta v_{i,n} + v_{i,n} = \frac{\frac{\partial \mathcal{H}}{\partial v_{i,n}} + \lambda v_{i,n}}{v_{i,n} \frac{\partial \mathcal{H}}{\partial v_{i,n}} + \lambda}, \quad i = 1, ..., N. \tag{13}$$

Here, λ is admissible iff $\lambda > |\frac{\partial \mathcal{H}}{\partial v_{i,n}}| \ \forall i, n$. In the next section, we present the generic form of the network objective function for the proposed neuron model, derive the corresponding updates for a non-spiking variant, and extend it to a stochastic form that leads to the model of a spiking neuron.

3 Growth Transform Neuron Model

Neurons react to synaptic inputs and external stimuli and propagate signals to other neurons by producing a rapid change in their transmembrane electrical potential difference, known as an action potential or a spike. Inputs result in the rapid depolarization and hyperpolarization of the membrane potential, thus generating spikes through the transient opening and closing of ion channels.

The proposed neuron model follows a similar process where each neuron tracks the net excitation it receives from other inputs or externally, while at the system-level, the network tries to minimize its overall energy. We consider a network of N neurons with the vector of state variables (i.e., membrane potentials) given by $\boldsymbol{v}$ and a synaptic weight matrix given by $\mathbf{Q} \in \mathcal{R}^N \times \mathcal{R}^N$, where Q_{ij} denotes the contribution of the response of the pre-synaptic neuron j to the net excitation received by the post-synaptic neuron i. The vector of external stimuli is denoted by $\mathbf{b} \in \mathcal{R}^N$. The network objective function (negative of the network energy) that is maximized by the Growth Transform neuron model is given by the following equation

$$\mathcal{H} = -\sum_{i=1}^{N} \int \Psi(v_i) dv_i - \sum_{i=1}^{N} \sum_{j=1}^{N} Q_{ij} v_j v_i + \sum_{i=1}^{N} b_i v_i. \tag{14}$$

For the non-spiking variant of the neuron model, we can define $\Psi(.)$ such that its integral $\int \Psi(v_i) dv_i$ over $[-1, 1]$ is a smooth and convex function. The steady-state first-order condition

$$(v_i^2 - 1) \frac{\partial \mathcal{H}}{\partial v} = 0 \tag{15}$$

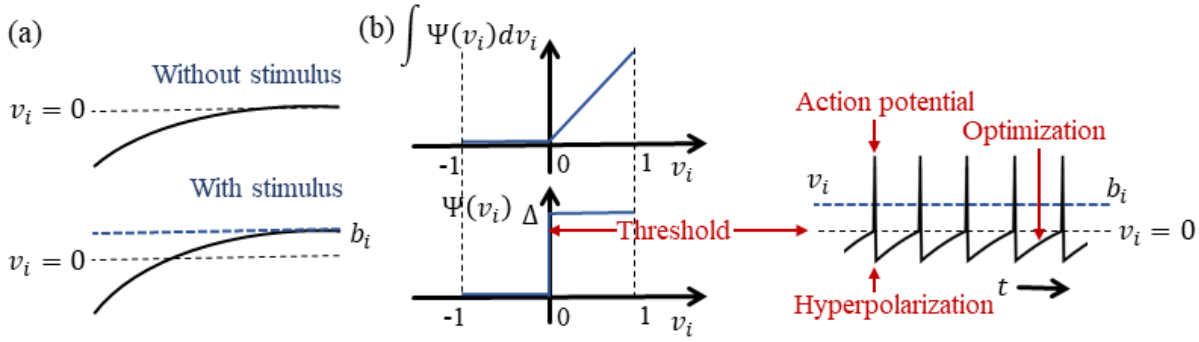

Figure 2: (a) Convergence of the response v_i of an uncoupled neuron in the absence and presence of external stimulus without the regularization function. (b) The regularization function and its derivative $\Psi(.)$ used in this paper, and time-evolution of the response v_i of an uncoupled neuron in the presence of external stimulus with the regularizer.

leads to the following response for the i-th neuron:

$$v_i = \begin{cases} \Psi^{-1}\left(\sum_j^N Q_{ij}v_j + b_i\right) & ; \quad |v_i| < 1 \\ 1 & ; \quad v_i \geq 1 \\ -1 & ; \quad v_i \leq -1 \end{cases} \tag{16}$$

We see that the nature and shape of the regularizer $\int \Psi(v_i)dv_i$ determines the response of the neuron given a particular input. It is possible to incorporate different non-linearities and response characteristics in the neuron model by changing this regularization function.

4 Growth Transform Spiking neuron model

For the spiking neuron model, $\Psi(.)$ is a spiking function with a gradient discontinuity at a pre-defined threshold that maps the neural response into a train of action potentials. We define an expectation operator $\mathcal{E}(.)$ for a discrete-time signal x_n as

$$\mathcal{E}_n(x_n) = \lim_{K\to\infty} \frac{1}{K} \sum_{n=1}^{K} x_n, \tag{17}$$

and for a continuous-time signal $x(t)$ as

$$\mathcal{E}_t(x(t)) = \lim_{T\to\infty} \frac{1}{T} \int_{t=0}^{T} x(t)dt. \tag{18}$$

If the regularization function given by (14) is made non-smooth over a subdomain of v_i, and if the critical point is not reachable by growth transform updates, some of the response variables v_i which are near the threshold will exhibit limit-cycle oscillations about the subdomain, while still maximizing the network objective (i.e., minimizing the network energy) on an average over time, thereby satisfying

$$\mathcal{E}_n\left[\frac{\partial \mathcal{H}}{\partial v_n}\right] \quad \rightarrow \quad 0, \quad \text{or} \tag{19}$$

$$\mathcal{E}_n\left[\Psi(v_{i,n})\right] \quad \rightarrow \quad \mathcal{E}_n\left[\sum_{j=1}^{N} Q_{ij}v_{j,n} + b_{i,n}\right] \tag{20}$$

(20) can be viewed as a stochastic variant of the first-order conditions given by (16), that minimizes the objective function in (14) over a time-average. A similar stochastic first-order framework was used in [17] to derive a dynamical system corresponding to $\Sigma\Delta$ modulation.

Rewriting (13) in terms of the objective function for the neuron model, we get

$$\frac{1}{f_{i,n}}\Delta v_{i,n} + v_{i,n} = g_i(\mathbf{v}_n), \;\; i = 1, ..., N, \tag{21}$$

where

$$g_i(\mathbf{v}_n) = \frac{-\sum_{j=1}^{N} Q_{ij} v_{j,n} + b_{i,n} - \Psi(v_{i,n}) + \lambda v_{i,n}}{-\sum_{j=1}^{N} Q_{ij} v_{j,n} v_{i,n} + b_{i,n} v_{i,n} - v_{i,n}\Psi(v_{i,n}) + \lambda}. \tag{22}$$

The spiking function $\Psi(.)$ used in this paper is given by

$$\Psi(v_{i,n}) = \begin{cases} \Delta & ; \;\; v_{i,n} > 0 \\ 0 & ; \;\; v_{i,n} \leq 0 \end{cases} \tag{23}$$

where Δ is a parameter that determines the degree of hyperpolarization following a spike. We first illustrate how the response v_i changes when a regularization term corresponding to this spiking function is added to the network objective. Fig. 2(a) shows the response of a single uncoupled neuron when there is no regularization function. Here, the response converges to the fixed point $v_i = 0$ in the absence of an external stimulus. When a stimulus comes, the fixed point shifts upward, leading to a new solution that is a function of the stimulus magnitude. The form of $\Psi(.)$ used to derive the results in this paper, and the corresponding regularization function are shown in Fig.2(b), along with the time-evolution of v_i, which changes when the regularization term is present. In the presence of external stimulus when the fixed point of the energy minimization process shifts upwards from zero, the gradient discontinuity at the threshold leads to a sharp transition in the response. Whenever v_i exceeds the threshold, a spike is added to the membrane potential trace, and the optimization process immediately brings v_i back to a state of 'hyperpolarization'.

Note that the operation of the neuron is governed by two sets of dynamics: (a) minimization of a network energy functional; (b) the modulation of the phase through the parameter $f_{i,n}$ that can be made time-varying and individually tunable for each neuron. Fortunately, the evolution of $f_{i,n}$ can be made as complicated as possible without affecting the asymptotic fixed-point of the optimization process. In the next section, we present a detailed overview of the neuron model and its parameters, and show how different forms of $f_{i,n}$ produce different sets of neuronal dynamics consistent with the dynamics that have been reported in neurobiology.

5 Neural Dynamics

Single neurons show a vast repertoire of response characteristics and dynamical properties that lend richness to their computational properties at the network level. Izhikevich in [13] provided an extensive review of different spiking neuron models and their ability to produce the different dynamics observed in biology. In this section, we show how we can reproduce a vast majority of such dynamics by changing the modulation function f in the neuron model, and extend these dynamics to build a coupled network with interesting properties like memory and global adaptation for energy-efficient neural representation. The results reported here are representative of the types of dynamical properties the proposed model can exhibit, but by no means exhaustive. Readers are encouraged to experiment with the software (MATLAB) implementation of the Growth Transform neuron model available through the web-portal at aimlab.seas.wustl.edu and try out different inputs and network parameters. The tool enables users to visualize the effects of different modulation functions and other hyperparameters on the neural dynamics, as well as the time-evolution of population trajectories and the network energy function with different inputs and under different initial conditions.

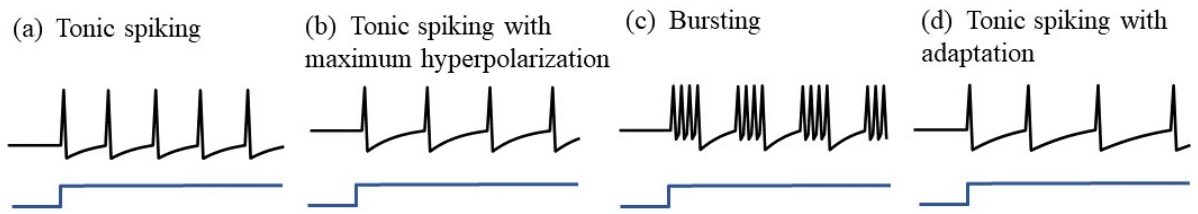

Figure 3: Simulations demonstrating different single-neuron responses obtained using the GT neuron model.

5.1 Standard uncoupled tonic-spiking response

At first, we present the results for an uncoupled network, with $Q_{ij} = \delta_{ij}, \ \forall i, j = 1, ..., N$. When stimulated with a constant DC current pulse, a vast majority of neurons fire single, repetitive action potentials for the duration of the stimulus, with or without adaptation [18, 19, 20]. The proposed model shows tonic spiking without adaptation when the modulation function $f_{i,n} = f$, where $0 < f \leq 1$. A simulation of tonic spiking response using the neuron model is given in Fig. 3(a).

5.2 Uncoupled tonic-spiking response with maximum hyperpolarization

The state of hyperpolarization reached by the neuron immediately after a spike can be tuned by varying the constant f, which regulates the speed of the growth transform updates at a particular point. The fastest rate at which the updates could take place corresponds to $f_{i,n} = 1$, leading to maximum hyperpolarization. The modulation function in this case is varied as follows

$$f_{i,n} = \begin{cases} f & ; \quad v_{i,n} < 0 \\ 1 & ; \quad v_{i,n} \geq 0 \end{cases} \tag{24}$$

Simulation for uncoupled tonic-spiking response with full after-polarization is given in Fig. 3(b) for the same input as in (a). It can be seen that the neuron reaches a more hyperpolarized state in this case, which increases the time required to reach the threshold once more, thus regulating the firing rate.

5.3 Uncoupled bursting response with maximum hyperpolarization

Bursting neurons fire discrete groups of spikes interspersed with periods of silence in response to a constant stimulus [18, 19, 21, 22]. Bursting arises from an interplay of fast ionic currents responsible for spiking, and slower intrinsic membrane currents that modulate the spiking activity, causing the neuron to alternate between activity and quiescence. Bursting response can be simulated in the proposed model by modulating $f_{i,n}$ at a slower rate compared to the generation of action potentials, in the following way

$$f_{i,n} = \begin{cases} f & ; \quad c_{i,n} < B \\ 1 & ; \quad c_{i,n} \geq B \end{cases} \tag{25}$$

where B is a hyper-parameter and the count variable $c_i(n)$ is updated according to

$$c_{i,n} = \begin{cases} c_{i,n-1} + \Psi(v_{i,n}) & ; \quad c_{i,n-1} < B \\ 0 & ; \quad c_{i,n-1} \geq B \end{cases} \tag{26}$$

Simulation of a bursting neuron in response to a step input is given in Fig. 3(c).

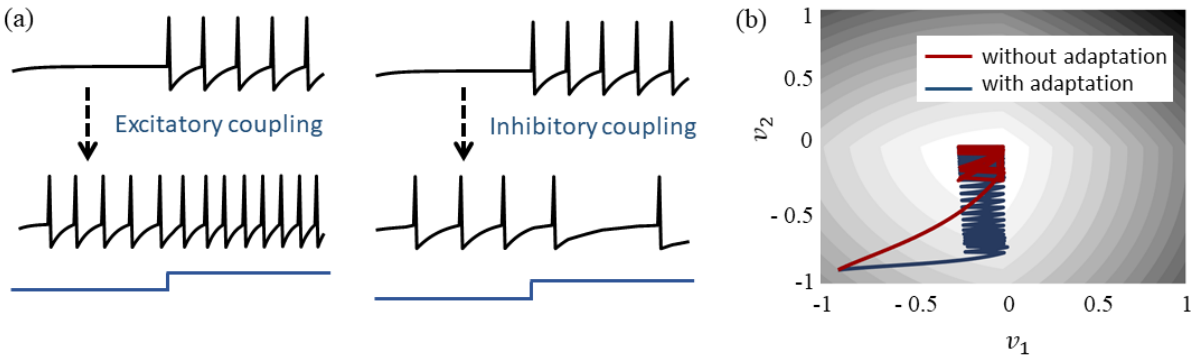

Figure 4: (a) Excitatory and inhibitory couplings using the model. (b) Different optimization conditions lead to different limit cycles within the same energy landscape.

5.4 Uncoupled tonic-spiking response with adaptation

When presented with a prolonged stimulus of constant amplitude, many cortical cells initially respond with a high-frequency spiking that decays to a lower steady-state frequency [23]. This adaptation in the firing rate is caused by a negative feedback to the cell excitability due to gradual inactivation of depolarizing currents or activation of slow hyperpolarizing currents upon depolarization, and occur at a time-scale slower than the rate of action potential generation. We modeled spike-frequency adaptation by varying the modulation function according to

$$f_{i,n} = \begin{cases} \sigma(-h_n * \Psi(v_{i,n})) & ; \quad v_{i,n} < 0 \\ 1 & ; \quad v_{i,n} \geq 0, \end{cases} \tag{27}$$

where $h_n * \Psi(v_{i,n})$ is a convolution operation between the time-domain filter h_n and the spiking function $\Psi(v_{i,n})$, and

$$\sigma(x) = b\left(1 + \frac{1}{1+\exp(-x)}\right) \tag{28}$$

is a sigmoidal function ensuring $1 > f_{i,n} > 0$. The parameter $b \in (0,1)$ determines the steady-state firing rate for a particular stimulus. For the results, the smoothing filter h_n has been chosen to be

$$H(z) = \frac{1}{1 - 0.99z^{-1} - 0.01\log_2(1+\beta)z^{-1}}, \tag{29}$$

where $\beta > 0$ is a hyper-parameter for tuning the filter. As the neuron spikes, f decreases, slowing down the growth-transform neuron updates until the frequency reaches a lower constant value. A tonic-spiking response with adaptation is shown in Fig. 3(d).

5.5 Coupled spiking network

We can extend the proposed framework to a network model where the neurons, apart from external stimuli, receive inputs from other neurons in the network. We begin by considering $\mathbf{Q}$ to be a positive-definite matrix, which gives an unique solution of (21). The modulation function, as before, is given by

$$f_{i,n} = \begin{cases} f & ; \quad v_{i,n} < 0 \\ 1 & ; \quad v_{i,n} \geq 0 \end{cases} \tag{30}$$

5.6 Coupled network with pre-synaptic adaptation

Interactions among the neurons in a coupled network can be captured by the modulation function as follows

$$f_{i,n} = \begin{cases} \sigma(h_n * \sum_j Q_{ij}\Psi(v_{j,n})) & ; \quad v_{i,n} < 0 \\ 1 & ; \quad v_{i,n} \geq 0 \end{cases} \tag{31}$$

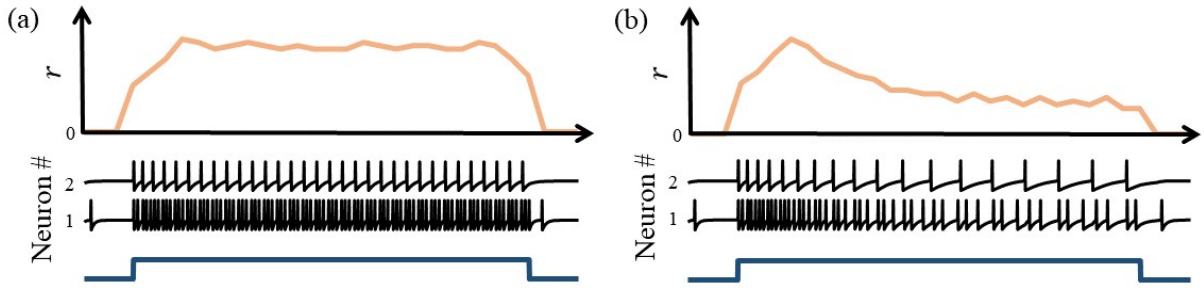

Figure 5: (a) Mean population firing rate and firing patterns in response to a step input without global adaptation. (b) Mean population firing rate and firing patterns in response to the same input when the global adaptation term is present.

with the compressive-function $\sigma(.)$ and smoothing-filter $h(n)$ given by (28) and (29). This ensures that $Q_{ij} > 0$ corresponds to an excitatory coupling from the pre-synaptic neuron j, and $Q_{ij} < 0$ corresponds to an inhibitory coupling, as demonstrated in Fig. 4(a). Fig. 4(b) illustrates how different variations of the modulation function under the same energy landscape leads to the neurons following different response trajectories and converging to varying limit-cycles. The energy contours for a two-neuron network corresponding to a particular $\boldsymbol{Q}$ and a fixed stimulus vector $\boldsymbol{b}$ are plotted, along with the responses of the two neurons starting from the same initial conditions, with and without pre-synaptic adaptation (where the latter corresponds to the case where neither neuron can integrate inputs from the other neuron). Because the energy landscape is the same in both cases, the neurons converge to the same sub-domain, but with widely varying trajectories and steady-state response patterns.

5.7 Coupled network with pre-synaptic and global adaptation for energy-efficiency

Apart from the pre-synaptic adaptation that changes individual firing rates based on the inputs received by each neuron, neurons in the coupled network can be made to adapt according to the global dynamics by changing the modulation function as follows

$$f_{i,n} = \begin{cases} \sigma(h_n * (\sum_j Q_{ij}\Psi(v_{j,n}) + \mathcal{F}(r,\dot{r}) & ; \quad v_{i,n} < 0 \\ 1 & ; \quad v_{i,n} \geq 0 \end{cases} \tag{32}$$

with the compressive-function $\sigma(.)$ and smoothing-filter h_n given by (28) and (29), where r denotes the mean firing rate of the population of neurons. The new function $\mathcal{F}(.)$ is used to capture the dynamics of the network cost-function. As the network starts to stabilize and converge to a fixed-point, the function $f_i(.)$ adapts to reduce the spiking rate of the neuron without affecting the steady-state solution. Fig.s 5(a) and (b) shows the time-evolution of the mean population firing rate and the spike-trains for a two-neuron network without global adaptation and with global adaptation respectively, using a form for the adaptation term as given below

$$\mathcal{F}(r,\dot{r}) = \begin{cases} -\sigma(h_n * c) & ; \quad r > 0 \text{ and } \dot{r} \approx 0 \\ 0 & ; \quad \text{otherwise,} \end{cases} \tag{33}$$

where c is a small constant. This feature is important in designing energy-efficient spiking networks where the energy is only dissipated during transients.

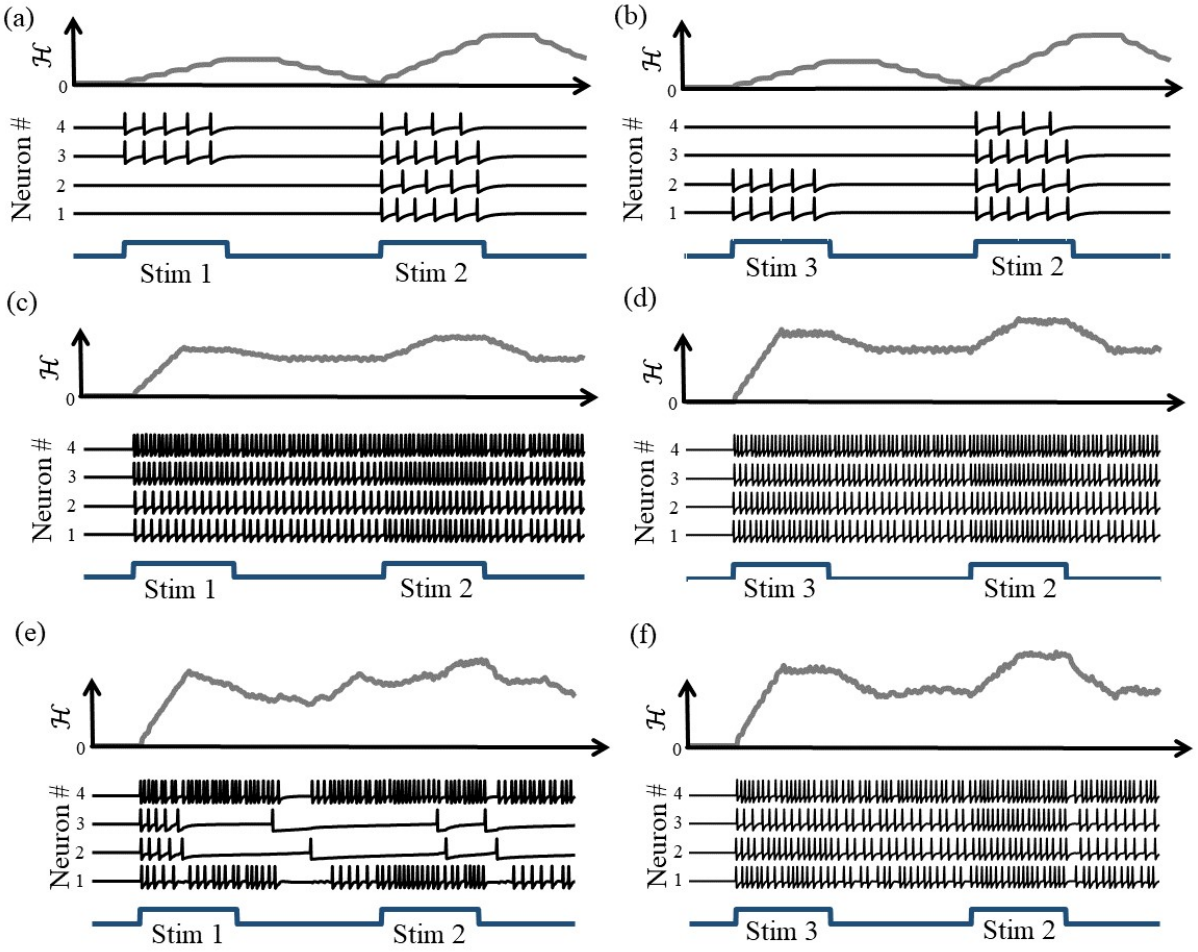

Figure 6: (a), (b) Response to stimulus 2 for an uncoupled network of 4 neurons following stimulus 1 and stimulus 3 respectively. (c), (d) Response to the same orders of stimuli for a coupled network with a positive definite Q. (e), (f) Response to the same orders of stimuli for a coupled network with a non-positive definite Q.

5.8 Coupled spiking network demonstrating memory

As illustrated in Fig. 6, a coupled spiking network can function as a memory element, when **Q** is a non-positive-definite matrix and

$$f_{i,n} = \begin{cases} f & ; \quad v_{i,n} < 0 \\ 1 & ; \quad v_{i,n} \geq 0 \end{cases} \tag{34}$$

Let us consider two different orders of stimulus presentation in a network of four neurons, where a stimulus 'Stim 1' precedes another stimulus 'Stim 2' in Fig.s 6(a), (c) and (e), and a third stimulus 'Stim 3' precedes 'Stim 2' in Fig.s 6(b), (d) and (f). Here, each 'stimulus' essentially corresponds to a different input vector $\boldsymbol{b}$. For an uncoupled network, where neurons do not receive any inputs from other neurons, the network energy increases when the first stimulus is applied, and returns to zero afterwards, and the network begins from the same state again for the second stimulus as for the first, leading to the same firing pattern for the second stimulus, as shown in Fig.s 6(a) and (b). For a coupled network with a positive definite synaptic weight matrix Q, reinforcing loops of spiking activity in the network may not allow the network energy to go to zero after the first stimulus is removed, and the residual energy makes the network exhibit a baseline activity that depends on stimulus history, as long as there is no dissipation. When the second stimulus is applied, the initial conditions for the network are different for the two stimulus histories, leading to two different transients until the network settles down into the same steady-state firing patterns, as shown in Fig.s 6(c) and (d). For a non-positive definite synaptic weight matrix Q however, depending on the initial condition, the network may settle down to different solutions for the same second stimulus, due to the possible presence of more than one local minimum. This leads to completely different transient as well as steady-state responses for the second stimulus, as shown in Fig. 6(e) and (f). This history-dependent stimulus response could serve as a short-term memory, where residual network energy from a previous external input subserves synaptic interactions among a population of neurons to set specific initial conditions for a future stimulus based on the stimulus history.

6 Conclusions

This paper introduces the theory behind a new spiking neuron model based on the Growth transform dynamical system, where an appropriate energy functional, when minimized under realistic physical constraints, produces emergent spiking activity in a population of neurons. The neuron model and its response are tightly coupled to the network objective, and is flexible enough to incorporate different neural dynamics that have been observed at the cellular level in electrophysiological recordings. In each of these experiments, the spiking activity is modulated externally by allowing a slower modulation function to evolve in different ways, without affecting the underlying optimization process. This allows the network to reach the same asymptotic fixed-point through many possible response trajectories, and using widely varying encoding techniques. The model can be easily extended to a coupled network of neurons, which can be tweaked to exhibit interesting properties like memory and global adaptation for energy-efficiency.

The paper is accompanied by a software tool that enables readers to visualize the effects of different model parameters on the neural dynamics. Many more neural dynamics can be simulated using the model and readers are encouraged to experiment with different network hyper-parameters. The paper and the tool illustrate how spike generation and spike-based encoding in an artificial neuron model can be framed as a network-level optimization problem, thereby providing a framework to develop scalable and energy-efficient neuromorphic machine learning algorithms. Currently, the model only considers fixed synaptic weights Q_{ij}. An interesting direction of future research would be to learn or adapt these weights for an optimal neural representation or encoding.

References

[1] E. M. Izhikevich, *Dynamical systems in neuroscience*. MIT press, 2007.

[2] A. L. Hodgkin and A. F. Huxley, "A quantitative description of membrane current and its application to conduction and excitation in nerve," *The Journal of physiology*, vol. 117, no. 4, pp. 500–544, 1952.

[3] R. FitzHugh, "Impulses and physiological states in theoretical models of nerve membrane," *Biophysical journal*, vol. 1, no. 6, pp. 445–466, 1961.

[4] E. M. Izhikevich, "Simple model of spiking neurons," *IEEE Transactions on neural networks*, vol. 14, no. 6, pp. 1569–1572, 2003.

[5] L. F. Abbott, "Lapicques introduction of the integrate-and-fire model neuron (1907)," *Brain research bulletin*, vol. 50, no. 5-6, pp. 303–304, 1999.

[6] H. R. Wilson and J. D. Cowan, "Excitatory and inhibitory interactions in localized populations of model neurons," *Biophysical journal*, vol. 12, no. 1, pp. 1–24, 1972.

[7] B. H. Jansen and V. G. Rit, "Electroencephalogram and visual evoked potential generation in a mathematical model of coupled cortical columns," *Biological cybernetics*, vol. 73, no. 4, pp. 357–366, 1995.

[8] G. N. Borisyuk, R. M. Borisyuk, A. I. Khibnik, and D. Roose, "Dynamics and bifurcations of two coupled neural oscillators with different connection types," *Bulletin of mathematical biology*, vol. 57, no. 6, pp. 809–840, 1995.

[9] W. Maass, T. Natschläger, and H. Markram, "Real-time computing without stable states: A new framework for neural computation based on perturbations," *Neural computation*, vol. 14, no. 11, pp. 2531–2560, 2002.

[10] D. J. Amit, H. Gutfreund, and H. Sompolinsky, "Storing infinite numbers of patterns in a spin-glass model of neural networks," *Physical Review Letters*, vol. 55, no. 14, p. 1530, 1985.

[11] Z. Jonke, S. Habenschuss, and W. Maass, "Solving constraint satisfaction problems with networks of spiking neurons," *Frontiers in neuroscience*, vol. 10, p. 118, 2016.

[12] A. Gangopadhyay and S. Chakrabartty, "Spiking, bursting, and population dynamics in a network of growth transform neurons," *IEEE transactions on neural networks and learning systems*, vol. 29, no. 6, pp. 2379–2391, 2018.

[13] E. M. Izhikevich, "Which model to use for cortical spiking neurons?" *IEEE transactions on neural networks*, vol. 15, no. 5, pp. 1063–1070, 2004.

[14] P. Gopalakrishnan, D. Kanevsky, A. Nadas, and D. Nahamoo, "A generalization of the baum algorithm to rational objective functions," in *Acoustics, Speech, and Signal Processing, 1989. ICASSP-89., 1989 International Conference on*. IEEE, 1989, pp. 631–634.

[15] O. Chatterjee and S. Chakrabartty, "Decentralized global optimization based on a growth transform dynamical system model," *IEEE Transactions on Neural Networks and Learning Systems*, 2018.

[16] L. E. Baum and G. Sell, "Growth transformations for functions on manifolds," *Pacific Journal of Mathematics*, vol. 27, no. 2, pp. 211–227, 1968.

[17] A. Gore and S. Chakrabartty, "A min-max optimization framework for designing σ learners: Theory and hardware," *IEEE Trans. Circuits Syst. I*, vol. 57, no. 3, pp. 604–617, 2010.

[18] A. Agmon and B. Connors, "Repetitive burst-firing neurons in the deep layers of mouse somatosensory cortex," *Neuroscience letters*, vol. 99, no. 1-2, pp. 137–141, 1989.

[19] D. A. McCormick, B. W. Connors, J. W. Lighthall, and D. A. Prince, "Comparative electrophysiology of pyramidal and sparsely spiny stellate neurons of the neocortex," *Journal of neurophysiology*, vol. 54, no. 4, pp. 782–806, 1985.

[20] J. R. Gibson, M. Beierlein, and B. W. Connors, "Two networks of electrically coupled inhibitory neurons in neocortex," *Nature*, vol. 402, no. 6757, p. 75, 1999.

[21] C. M. Gray and D. A. McCormick, "Chattering cells: superficial pyramidal neurons contributing to the generation of synchronous oscillations in the visual cortex," *Science*, vol. 274, no. 5284, pp. 109–113, 1996.

[22] J. C. Brumberg, L. G. Nowak, and D. A. McCormick, "Ionic mechanisms underlying repetitive high-frequency burst firing in supragranular cortical neurons," *Journal of Neuroscience*, vol. 20, no. 13, pp. 4829–4843, 2000.

[23] B. W. Connors and M. J. Gutnick, "Intrinsic firing patterns of diverse neocortical neurons," *Trends in neurosciences*, vol. 13, no. 3, pp. 99–104, 1990.